

# SCN5A mutation (T1620M) causing Brugada syndrome exhibits different phenotypes when expressed in *Xenopus* oocytes and mammalian cells

Ghayath Baroudi<sup>a</sup>, Eric Carbonneau<sup>a</sup>, Valérie Pouliot<sup>b</sup>, Mohamed Chahine<sup>a,b,\*</sup>

<sup>a</sup>Laval University, Department of Medicine, Sainte-Foy, Que. G1K 7P4, Canada

<sup>b</sup>Québec Heart Institute, Laval Hospital, Research Center, 2725 Chemin Sainte-Foy, Sainte-Foy, Que. G1V 4G5, Canada

Received 22 November 1999

Edited by Maurice Montal

**Abstract** Brugada syndrome is a hereditary cardiac disease causing abnormal ST segment elevation in the ECG, right bundle branch block, ventricular fibrillation and sudden death. In this study we characterized a new mutation in the *SCN5A* gene (T1620M), causing the Brugada syndrome. The mutated channels were expressed in both *Xenopus leavis* oocytes and in mammalian tsA201 cells with and without the  $\beta$ -subunit and studied using the patch clamp technique. Opposite phenotypes were observed depending on the expression system. T1620M mutation led to a faster recovery from inactivation and a shift of steady-state inactivation to more positive voltages when expressed in *Xenopus* oocytes. However, using the mammalian expression system no effect on steady-state inactivation was observed, but this mutation led to a slower recovery from inactivation. Our finding supports the idea that the slower recovery from inactivation of the cardiac sodium channels seen in our mammalian expression system could decrease the density of sodium channels during the cardiac cycle explaining the in vivo arrhythmogenesis in patients with Brugada syndrome.

© 2000 Federation of European Biochemical Societies.

**Key words:** Brugada syndrome; Ventricular fibrillation; Sodium channel; Cardiac muscle; Electrophysiology; *SCN5A*

## 1. Introduction

Ventricular fibrillation is the most common cause of sudden death, with more than 300 000 deaths per year in the USA alone [1,2]. Brugada syndrome is a hereditary cardiac disease characterized by a right bundle-branch block (RBBB), an elevation of the ST segment in leads V1 through V3 on the ECG and a ventricular fibrillation (VF) that can lead to sudden death [3]. The incidence of the Brugada syndrome is greatest in Asian males. It is a major cause of death in Japan (6:1000) and much of southeast Asia. The syndrome is a leading cause of death of young males in Thailand (1:2500) [4]. The age for the first arrhythmic event ranges between 2 and 77 years, with a mean age of 35–41 years [4–6]. In contrast to Long QT syndrome (LQTS), QTc is not affected in the Brugada syndrome.

Until now, Brugada syndrome has been associated with only one gene, *SCN5A*. The gene encodes the  $\alpha$ -subunit of human cardiac voltage-gated sodium channel and is located on chromosome 3 [7]. In patients with Brugada syndrome, missense T1620M [8] and R1512W [9], splice-donor, and

frameshift mutations have been identified in *SCN5A* [8]. The insertion of a pair of adenosines disrupts the splice-donor sequence of intron 7 [10], and the deletion of a single nucleotide (A) at codon 1397 results in an in-frame stop codon that eliminates DIII/S6, DIV/S1-S6, and the carboxy-terminal portion of the cardiac sodium channel [8]. The T1620M mutation was expressed and characterized by Chen and coworkers [8] in *Xenopus* oocytes. In their study, mutant sodium channel (T1620M) showed faster recovery from inactivation in comparison with the wild-type (WT) cardiac sodium channel and a shift of the steady-state inactivation curve to more positive potentials. In particular, unlike *SCN5A* mutations associated with long QT syndrome, no persistent inactivation-resistant currents were observed in the mutated channel [8]. Functional analysis of the mutant channels have provided a mechanistic explanation for this elevation of the T-wave in the ECG of Brugada syndrome patients [11]. It has been suggested [11] that heterogeneity of repolarization between endocardial and epicardial layers could be responsible for the clinical manifestation of the Brugada syndrome. In contrast to endocardial cells, action potentials of epicardial cells display a pronounced phase 1 due to the transient outward current,  $I_{to}$ , which is preferentially expressed in the epicardium rather than in the endocardium of the ventricles of many species, including humans [12]. This underlies the difference in the endocardial-epicardial action potential (AP) configurations. Recent studies also indicate the presence of a much larger transient outward current  $I_{to}$  in the right versus the left ventricular epicardium [13] which can explain ECG patterns on the right leads. Perturbations in sodium  $I_{Na}$  and/or transient  $I_{to}$  currents can lead to a striking abbreviation of the epicardial AP, with the resultant potential for reexcitation due to the epicardial-endo-cardial heterogeneity of repolarization [14].

In this work, we expressed and characterized the T1620M mutant cardiac sodium channels in two different expression systems, *Xenopus* oocytes and tsA201 mammalian cells. The mutant channel showed different electrophysiological properties in each system. Our results implicate the electrophysiological characteristics of the mutated cardiac sodium channel hH1/T1620M expressed in mammalian cells as a major cause of VF and the ST segment elevation in the ECG of Brugada syndrome patients.

## 2. Materials and methods

### 2.1. Mutagenesis

Mutant hH1/T1620M was generated using QuickChange™ site-directed mutagenesis kit manual instruction from Stratagene (La Jolla, CA, USA) according to the manufacturer's instructions. The

\*Corresponding author. Fax: (1)-418-656 4509.  
E-mail: mohamed.chahine@phc.ulaval.ca

mutations were constructed using the following mutagenic sense and antisense primers: 5'-GTA CTT CTT CTC CCC GAT GCT CTT CCG AGT CAT CC-3' and 5'-GGA TGA CTC GGA AGA GC<sub>4</sub> CCG GGG AGA AGA AGT AC-3' for hH1/T1620M. The underlined nucleotides represent mutated sites.

Mutant and the WT hH1 in pcDNA1 construct were purified using Quiagen columns (Quiagen Inc., Chatsworth, CA, USA).

The human sodium channel  $\beta 1$  subunit in pRc/CMV vector was provided by Dr. A.L. Georges (Vanderbilt University, Nashville, TN, USA).

## 2.2. Transfections of the tsA201 cell line

The mammalian cell line tsA201 is derived from human embryonic kidney HEK293 cells by stable transfection with SV40 large T antigen. Cells were grown in high glucose DMEM (Dulbecco's modified Eagle's medium) supplemented with 10% FBS, L-glutamine (2 mM), penicillin G (100 U/ml) and streptomycin (10 mg/ml) (Gibco BRL Life technologies, Burlington, Ont., Canada). Cells were incubated in a 5% CO<sub>2</sub> humidified atmosphere. The tsA201 cells were transfected using the calcium phosphate method, with the following modification: to better identify the individual transfected cells, 10  $\mu$ l of a CD8-a (lymphocyte surface antigen) plasmid was cotransfected with 10  $\mu$ l of either the WT or mutant hH1 sodium channels cDNA. For the patch clamp experiments, 2 to 3 days post-transfection cells were incubated for 2 min in a medium containing anti-CD8-a coated beads (Dyna-beads M-450 CD8-a). The unattached beads were removed by washing. Beads were prepared according to the manufacturer's instructions (DynaL A.S., Oslo, Norway). Cells expressing CD8-a on their surface fixed the beads and were distinguished from non-transfected cells by light microscopy.

## 2.3. Patch clamp methods

Macroscopic sodium currents from transfected cells were recorded using the whole-cell configuration of the patch clamp technique. Patch electrodes were made from 8161 Corning glass and coated with Sylgard (Dow-Corning, Midland, MI, USA) to minimize their capacitance. Low resistance electrodes (<0.8 M $\Omega$ ) were used, and a routine series resistance compensation of an Axopatch 200 amplifier was performed to values >80% to minimize voltage-clamp errors. Voltage-clamp command pulses were generated by microcomputer using pCLAMP software v5.5 (Axon Instruments, Foster City, CA, USA). Recorded membrane currents were filtered at 5 kHz. Experiments were performed 10 min after obtaining the whole-cell configuration to allow the current to stabilize.

## 2.4. Solutions and reagents

For whole-cell recording, the patch pipette contained: 35 mM NaCl; 105 mM CsF; 10 mM EGTA; and 10 mM Cs-HEPES (pH 7.4). The bath solution contained: 150 mM NaCl; 2 mM KCl; 1.5 mM CaCl<sub>2</sub>; 1 mM MgCl<sub>2</sub>; 10 mM glucose and 10 mM Na-HEPES (pH 7.4). A correction of the liquid junction potential of -7 mV between patch pipette and the bath solutions was made. Experiments were performed at ambient temperature (22–23°C).

## 2.5. Expression in *Xenopus* oocytes

*Xenopus laevis* females were anesthetized with 1.5 mg/ml tricaine (Sigma), and two or three ovarian lobes were surgically removed. Follicular cells surrounding the oocytes were removed by incubation at 22°C for 2.5 h in calcium-free oocyte medium (82.5 mM NaCl, 2.5 mM KCl, 1 mM MgCl<sub>2</sub>, 5 mM Na-HEPES, pH 7.6) containing 2 mg/ml collagenase (Sigma, type 1A). The oocytes were washed first in calcium-free medium with a 50% diluted solution of Leibovitz's L-15 medium (Gibco) enriched with 15 mM Na-HEPES, 5 mM L-glutamine, and 10 mg/ml gentamicin (pH 7.6); oocytes were stored in this medium until use. Stage V-VI oocytes were selected and micro-injected with cRNA encoding the WT and the mutant hH1. Oocytes were used for experiments after 3–5 days.

The macroscopic Na<sup>+</sup> currents from cRNA-injected oocytes were measured by two-microelectrode voltage clamp. The cells were impaled with <1.5 M $\Omega$  electrodes containing 3 M KCl and were voltage-clamped with an OC-725 Oocyte clamp (Warner Instruments, Hamden, CT, USA). The Ringer solution bath contained: 116 mM NaCl; 2 mM KCl; 1.8 mM CaCl<sub>2</sub>; 2 mM MgCl<sub>2</sub>; 5 mM Na-HEPES (pH 7.6). The holding potential was set between -110 mV and -80 mV in different experiments. Data were collected and analyzed using

pCLAMP software v7 (Axon Instruments). The inactivation data were fitted by Boltzmann equation and the recovery data were fitted by exponential function.

## 2.6. Statistical analysis

Data are expressed as mean  $\pm$  S.E.M. (standard error of the mean).

When indicated, *t*-test was performed using statistical software in SigmaPlot (Jandel Scientific Software, San Rafael, CA, USA). Differences were deemed significant at a *P* value < 0.05.

## 3. Results

### 3.1. Expression in *Xenopus laevis* oocytes

Both mutated (T1620M) and WT cardiac sodium channels hH1 were expressed and studied in *Xenopus* oocytes (Fig. 1). Large sodium currents were recorded from both hH1/WT and hH1/T1620M mutant channels, indicating that the level of expression was not affected by the mutation. As can be seen from Fig. 1 the decay of sodium currents were not affected by T1620M mutation. The voltage-dependence of the steady-state inactivation was studied using a two-pulse protocol and shown to be shifted by nearly 10 mV towards more positive potentials compared with WT channels (Fig. 2A). The normalized peak current was fitted to a Boltzmann distribution. The half-inactivation voltages were respectively  $-67.9 \pm 0.6$  mV ( $n=8$ ) and  $-77.5 \pm 0.8$  mV ( $n=8$ ) in mutant T1620M and WT channel. The slope factors were not significantly changed. The T1620M mutation did not induce any persistent inward currents (data not shown). The recovery from inactivation was assessed using a double-pulse protocol and time course of recovery from inactivation was measured. The time constant of recovery from inactivation was accelerated. For example, time constants of recovery from fast inactivation measured at -80 mV for T1620M mutant ( $n=8$ ) and the WT ( $n=8$ ) channel were  $23.5 \pm 0.8$  ms versus  $38.3 \pm 1.4$  ms, respectively and  $7.1 \pm 0.2$  ms versus  $9.3 \pm 0.4$  ms at -100 mV (Fig. 2B).

Channels (mutant T1620M and WT) were then coexpressed with the  $\beta$  regulatory subunit of the cardiac sodium channel and characterized in *Xenopus* oocytes. Neither mutated nor normal channels showed significant difference in the voltage dependence of steady-state inactivation when coexpressed with the  $\beta$ -subunit (Fig. 2A). However, in T1620M mutants, the inactivation curve was shifted toward a more positive potentials (with and without the  $\beta$ -subunit). Time constants of recovery from inactivation were accelerated, for example,

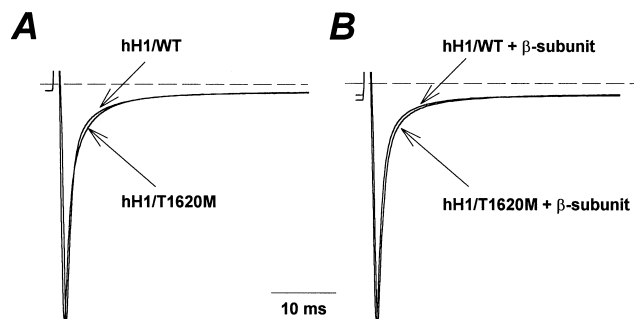


Fig. 1. Representative voltage clamp recording made from oocytes expression hH1/WT and hH1/T1620M (A) and coexpressed with the  $\beta$ -subunit (B). Normalized and superimposed current traces were obtained at test potential of -30 mV from a holding potential of -120 mV are shown.

at holding potential of  $-80$  mV,  $\tau_{\text{rec}} = 19.6 \pm 1.9$  ms and  $30.5 \pm 1.2$  ms for mutant T1620M and normal channels, respectively ( $n = 8$ ). The  $\tau_{\text{rec}}$  from channels coexpressed with the  $\beta$ -subunit was further accelerated (Fig. 2B).

### 3.2. Expression in tsA201 cells

Similar experiments were performed in a mammalian expression system, the tsA201 cell line. First, mutant and normal channels were expressed separately and studied. Second, both normal and mutant were coexpressed with the  $\beta$ -subunit. Elevated currents were recorded from both WT and mutant channels (Fig. 3). Peak conductance-voltage plots that represent steady-state activation (Fig. 4A) in mutated hH1/T1620M channels were indistinguishable from the hH1/WT. Steady-state inactivation was studied using the double-pulse protocol. No significant changes were observed on the steady-state inactivation curve of the mutant hH1/T1620M channels. In the presence of the  $\beta$ -subunit, the steady-state inactivation curves of both hH1/T1620M and hH1/WT were significantly shifted by 10 mV toward more positively charged holding potentials, with no significant changes in the slope of the curves ( $P < 0.05$ ) (Fig. 4A);  $V_{1/2 \text{ hH1/T1620M}} = -101.02 \pm 1.4$  mV ( $n = 17$ ) compared to  $V_{1/2 \text{ hH1/WT}} = -101.06 \pm 1.2$  mV ( $n = 22$ ). However, when recovery from fast inactivation was studied, T1620M mutant channels, expressed alone or in the presence of the  $\beta$  regulatory subunit, showed slower recovery

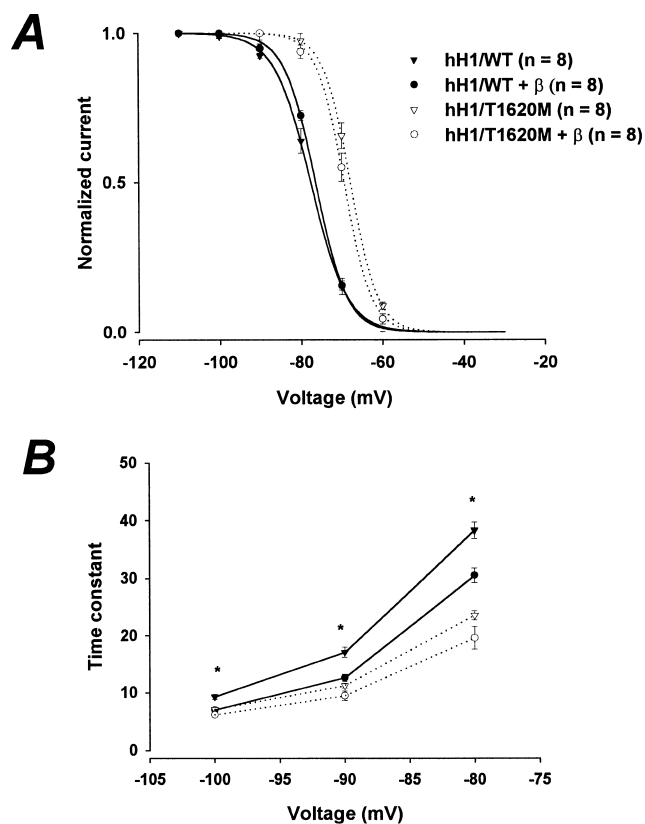


Fig. 2. Voltage-dependence of inactivation and time course of recovery from inactivation of hH1 WT and mutants channels expressed in *Xenopus* oocytes. A: Voltage-dependence of steady-state inactivation ( $I_{\infty}$ ) of hH1, WT and mutant, at  $-30$  mV triggered by 500 ms pulse ranged from  $-100$  mV to  $-30$  mV. The curves were fitted to a Boltzmann distribution  $I/I_{\text{max}} = 1/(1 + \exp((V - V_{1/2})/K_v))$ . B: Voltage-dependence of the time constant of recovery from inactivation.

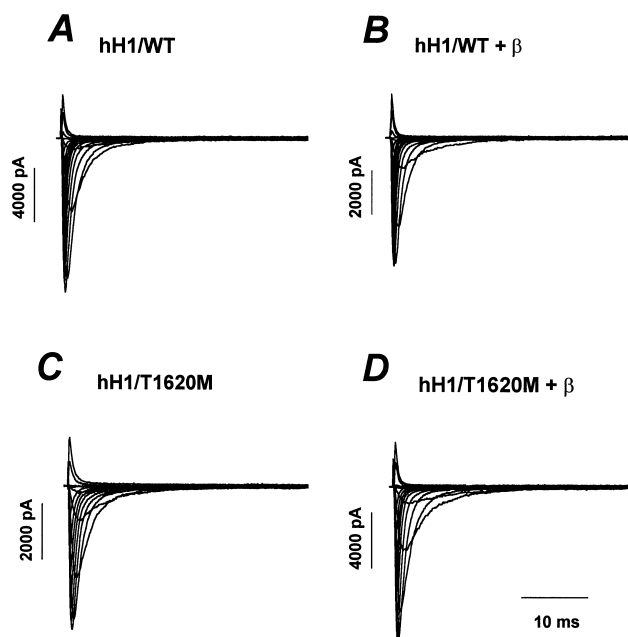


Fig. 3. Whole-cell sodium current traces from hH1/WT (A), hH1/WT +  $\beta$ -subunit (B), hH1/T1620M (C) and hH1/T1620M +  $\beta$ -subunit (D) expressed in the tsA201 cell line. Currents were recorded from a holding potential of  $-120$  mV stepped from  $-80$  mV to  $+60$  mV during 30 ms in 10 mV increments.

from fast inactivation (Fig. 4B). The mutant hH1/T1620M alone and hH1/T1620M coexpressed with the  $\beta$  regulatory subunit were compared to the wild-type hH1/WT and hH1/WT coexpressed with the  $\beta$ -subunit, respectively. At a holding potential of  $-100$  mV, the recovery from fast inactivation was 11.8% slower in cells expressing mutant channels alone than the WT, and 27.8% slower in cells co-expressing mutants with the  $\beta$ -subunit compared to the WT coexpressed with the  $\beta$ -subunit, for example,  $\tau_{\text{rec hH1/T1620M}} = 61.16 \pm 3.2$  ms ( $n = 14$ ) vs.  $\tau_{\text{rec hH1/WT}} = 53.96 \pm 4.2$  ms ( $n = 22$ ) and  $\tau_{\text{rec hH1/T1620M} + \beta} = 50.87 \pm 3.78$  ms ( $n = 12$ ) versus  $\tau_{\text{rec hH1/WT} + \beta} = 36.75 \pm 3.8$  ms ( $n = 21$ ). At more negative holding potentials, mutants showed a significantly ( $P < 0.05$ ) slower recovery from inactivation both in the presence and the absence of the  $\beta$ -subunit (Fig. 4C).

## 4. Discussion

In a previous study, Chen et al. identified a Brugada syndrome mutation (T1620M) and its electrophysiological characterization in *Xenopus* oocytes expression system was reported [8]. They showed that the voltage dependence of the steady-state inactivation was shifted by nearly 10 mV towards more positive potentials in T1620M mutated channels compared to the WT channels, with no change in the slope of the curve. Recovery from inactivation was significantly faster in mutated than in WT channels. In this study we compared and characterized the cardiac sodium channel missense mutation T1620M after its expression in both *Xenopus leavis* oocytes and mammalian tsA201 cells, with and without the  $\beta$ -subunit

Our first observation was that the expression of the human cardiac sodium channel was different in the two experimental systems tested. In fact, opposite phenotypes were observed depending upon the expression system. Our results in *Xenopus*

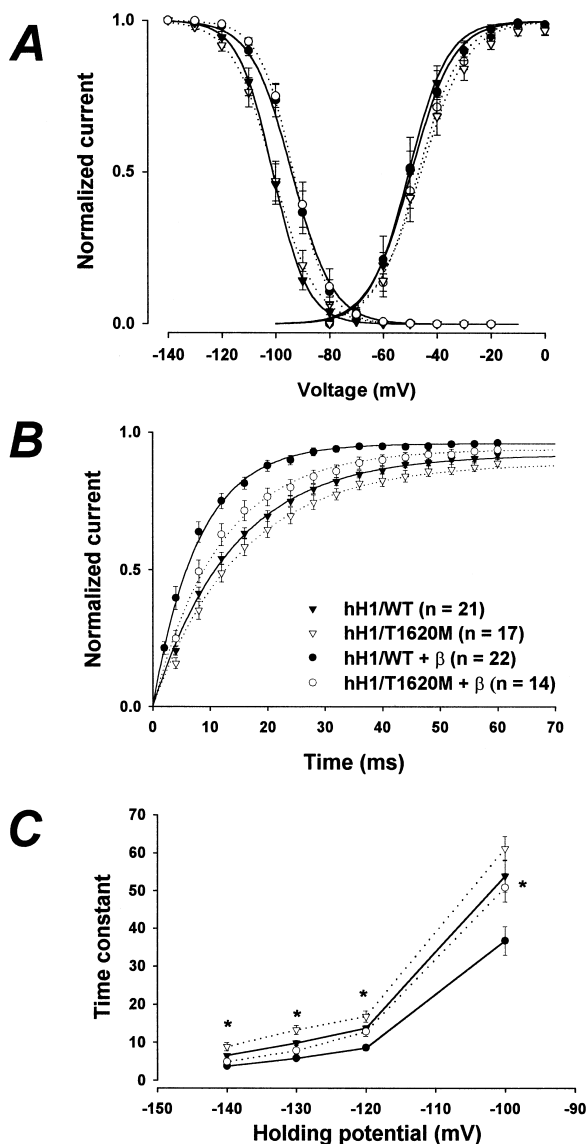


Fig. 4. Voltage-dependence of activation and inactivation, and time course of the recovery from inactivation of hH1 WT and mutant channels expressed in tsA201 cells. A: Steady-state voltage-dependence of activation and inactivation in normal and mutated sodium channels fitted to Boltzmann distributions. B: Time course of recovery from inactivation was studied using a two-pulse protocol of  $-20$  mV measured at various interpulse intervals  $\Delta t$ , at  $-120$  mV holding potential. The straight lines represent the fit obtained using the following equation  $I_{\text{test}}/I_{\text{pre-pulse}} = 1 - \exp(-t/\tau_{\text{rec}})$ . C: Voltage-dependence of recovery from inactivation \*: mutants are significantly different from the WT channel ( $P < 0.005$ ).

oocytes were consistent with those reported by Chen et al. [8]. The steady-state inactivation peak currents in the mutated channels were shifted by 10 mV toward more positive potentials in comparison to the WT channels in the *Xenopus leavis* oocytes system and in both cases (with and without the  $\beta$ -subunit); however, there was no shift in the mammalian expression system. Recovery from fast inactivation in oocytes was faster in the case of mutated channels hH1/T1620M although it showed slower recovery in the mammalian expression system (tsA201 cells).

Our results also show that coexpression of both channels (WT and mutant) with the  $\beta$ -subunit further accelerates time

constants of the recovery from fast inactivation. These observations indicate that the regulatory  $\beta$ -subunit plays an important role in modulating the human cardiac sodium channel.

In a recent study, Dumaine and coworkers found that at room temperature the recovery from fast inactivation was slightly faster in T1620M mutant than at  $32^\circ\text{C}$  [15]. We observed a slower recovery from inactivation at room temperature and even slower when the  $\beta$ -subunit was present. The cause of this discrepancy is not clear. We think that working at a higher temperature should result in qualitatively similar results (slowing of recovery from inactivation).

This suggests another explanation for the implication of the cardiac sodium channel in the Brugada syndrome and its ECG patterns. It could be that the human cardiac sodium channel protein expressed and studied in a mammalian derived expression system more closely approximates the in vivo arrhythmic cases given the similarities in the cellular metabolism and the environmental circumstances between the human ventricular myocytes and the tsA201 mammalian cells.

Observations and hypothesis postulated in previous studies support the idea that the 50% loss of functional cardiac sodium channels in the human heart results from the premature in-frame stop codon in the DIII-S6 region of the human cardiac sodium channel and that this is the cause of the shorter duration of the AP in epicardial cells [8]. This shortening is related to the presence of the transient outward current,  $I_{\text{to}}$ , which is more prominent in epicardial than endocardial myocytes [12]. Also, several reports of the pharmacological effects of drugs that block the sodium channel have indicated that treatment with class IA inactivated-state blockers (disopyramide, procainamide, flecainide and ajmaline) increased ST-segment elevation [16–18] in patients both with transient normalized ECGs and in the family members with normal ECGs. In summary, our data suggest that the characteristically elevated ST-segment appearing on the ECG of patients with Brugada syndrome is most probably due to the slower recovery from inactivation of the cardiac sodium channels. This can be explained by the presence of the T1620M which abolishes the opposing current (inward  $\text{Na}^+$  current) during the cardiac cycle in patients carrying this mutation.

**Acknowledgements:** This study was supported by the Heart and Stroke Foundation of Québec, the Medical Research Council of Canada MT-13181. Dr. M. Chahine is Research Scholar of the Heart and Stroke Foundation of Canada.

## References

- [1] Kannel, W.B., Cupples, L.A. and D'Agostino, R.B. (1987) Am. Heart J. 113, 799–804.
- [2] Willich, S.N., Levy, D., Rocco, M.B., Tofler, G.H., Stone, P.H. and Muller, J.E. (1987) Am. J. Cardiol. 60, 801–806.
- [3] Brugada, P. and Brugada, J. (1992) J. Am. Coll. Cardiol. 20, 1391–1396.
- [4] Nademanee, K. (1997) Am. J. Cardiol. 79, 10–11.
- [5] Brugada, J., Brugada, R. and Brugada, P. (1998) Circulation 97, 457–460.
- [6] Marcus, F.I. (1997) J. Cardiovasc. Electrophysiol. 8, 1075–1083.
- [7] George, A.L.J., Varkony, T.A., Drabkin, H.A., Han, J., Knops, J.F., Finley, W.H., Brown, G.B., Ward, D.C. and Haas, M. (1995) Cytogenet. Cell Genet. 68, 67–70.
- [8] Chen, Q., Kirsch, G.E., Zhang, D., Brugada, R., Brugada, J., Brugada, P., Potenza, D., Moya, A., Borggrefe, M., Breithardt, G., Ortiz-Lopez, R., Wang, Z., Antzelevitch, C., O'Brien, R.E.,

- Schulze-Bahr, E., Keating, M.T., Towbin, J.A. and Wang, Q. (1998) *Nature* 392, 293–296.
- [9] Deschênes, I., Baroudi, G., Barde, I., Berthet, T., Chalvidan, T., Denjoy, I., Guicheney, P. and Chahine, M. (2000) *Cardiovas. Res.*, in press.
- [10] Wang, Q., Li, Z., Shen, J. and Keating, M.T. (1996) *Genomics* 34, 9–16.
- [11] Alings, M. and Wilde, A. (1999) *Circulation* 99, 666–673.
- [12] Litovsky, S.H. and Antzelevitch, C. (1989) *J. Am. Coll. Cardiol.* 14, 1053–1066.
- [13] Di Diego, J.M., Sun, Z.Q. and Antzelevitch, C. (1996) *Am. J. Physiol.* 271, H548–H561.
- [14] Antzelevitch, C., Sicouri, S., Litovsky, S.H., Lukas, A., Krishnan, S.C., Di Diego, J.M., Gintant, G.A. and Liu, D.W. (1991) *Circ. Res.* 69, 1427–1449.
- [15] Dumaine, R., Towbin, J.A., Brugada, P., Vatta, M., Nesterenko, D.V., Nesterenko, V.V., Brugada, J., Brugada, R. and Antzelevitch, C. (1999) *Circ. Res.* 85, 803–809.
- [16] Nademanee, K., Veerakul, G., Nimmannit, S., Chaowakul, V., Bhuripanyo, K., Likittanasombat, K., Tunsanga, K., Kuasirikul, S., Malasit, P., Tansupasawadikul, S. and Tatsanavivat, P. (1997) *Circulation* 96, 2595–2600.
- [17] Miyazaki, T., Mitamura, H., Miyoshi, S., Soejima, K., Aizawa, Y. and Ogawa, S. (1996) *J. Am. Coll. Cardiol.* 27, 1061–1070.
- [18] Brugada, J. and Brugada, P. (1997) *J. Cardiovasc. Electro-physiol.* 8, 325–331.